$g-2$ of the Muon: Theory and Experiment Challenge One Another

B. Ananthanarayan
Centre for High Energy Physics, Indian Institute of Science
Bangalore 560 012, India

Precession in a magnetic field

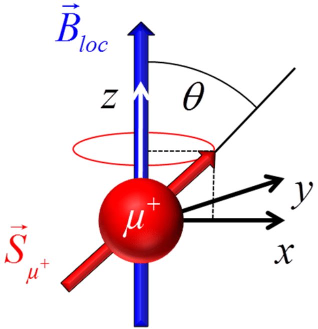

Outline

1. Introduction
2. A little about Quantum Electrodynamics
3. $g-2$ of the muon: some history and status
4. Theoretical Challenges in hadronic vacuum polarization and hadronic light by light scattering
5. The Brookhaven and Fermilab Experiment
6. Review of our work on form factor determination
7. Conclusions and Outlook

- Muon is an elementary particle and is like the electron in all respects except for being about 210 times heavier
- Decays via the charged current weak interaction into an electron and a pair of neutrinos $\mu \to e\nu_e\nu_\mu$ with a lifetime of approximately 2 microseconds in its rest frame
- Obviously interacts electromagnetically since it is charged. No electric dipole moment measured since it would be a signal of leptonic CP violation. Arises at higher orders in the weak interactions due to the CKM phase, but immeasurably small
- Fermilab measurement $11659\,2040(54) \times 10^{-11}$ (0.46 ppm) [3.3 σ]
- BNL measurement $11659\,2080(54)(33) \times 10^{-11}$
- Theory (White Paper) $11659\,1810(43) \times 10^{-11}$

Cartoon of muon $g-2$

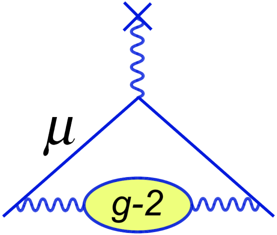

Recall that $1/\alpha \simeq 137.05$ and $\alpha/(2\pi) \simeq 0.00116$

Schwinger Headstone

Important Publications

- G. W. Bennett *et al.* Muon g-2 Collaboration, Phys. Rev. D **73** (2006), 072003 doi:10.1103/PhysRevD.73.072003 [arXiv:hep-ex/0602035 [hep-ex]].
- T. Albahri *et al.* Muon g-2 Collaboration, "Beam dynamics corrections to the Run-1 measurement of the muon anomalous magnetic moment at Fermilab," Phys. Rev. Accel. Beams **24** (2021) no.4, 044002 doi:10.1103/PhysRevAccelBeams.24.044002 [arXiv:2104.03240 [physics.acc-ph]].
- B. Abi *et al.* Muon g-2 Collaboration, "Measurement of the Positive Muon Anomalous Magnetic Moment to 0.46 ppm," Phys. Rev. Lett. **126** (2021) no.14, 141801 doi:10.1103/PhysRevLett.126.141801 [arXiv:2104.03281 [hep-ex]].
- T. Albahri *et al.* Muon g-2 Collaboration, "Magnetic-field measurement and analysis for the Muon g2 Experiment at Fermilab," Phys. Rev. A **103** (2021) no.4, 042208 doi:10.1103/PhysRevA.103.042208 [arXiv:2104.03201 [hep-ex]].
- T. Albahri *et al.* Muon g-2 Collaboration, "Measurement of the anomalous precession frequency of the muon in the Fermilab Muon g2 Experiment," Phys. Rev. D **103** (2021) no.7, 072002 doi:10.1103/PhysRevD.103.072002 [arXiv:2104.03247 [hep-ex]].

- T. Aoyama, N. Asmussen, M. Benayoun, J. Bijnens, T. Blum, M. Bruno, I. Caprini, C. M. Carloni Calame, M. Cè and G. Colangelo, *et al.* "The anomalous magnetic moment of the muon in the Standard Model," Phys. Rept. **887** (2020), 1-166 doi:10.1016/j.physrep.2020.07.006 [arXiv:2006.04822 [hep-ph]].
- J. P. Miller, E. de Rafael, B. L. Roberts and D. Stöckinger, "Muon (g-2): Experiment and Theory," Ann. Rev. Nucl. Part. Sci. **62** (2012), 237-264 doi:10.1146/annurev-nucl-031312-120340
- F. Jegerlehner, "The Anomalous Magnetic Moment of the Muon," Springer Tracts Mod. Phys. **274** (2017), pp.1-693 doi:10.1007/978-3-319-63577-4
- T. Aoyama, M. Hayakawa, T. Kinoshita and M. Nio, "Tenth-Order QED Contribution to the Electron g-2 and an Improved Value of the Fine Structure Constant," Phys. Rev. Lett. **109** (2012), 111807 doi:10.1103/PhysRevLett.109.111807 [arXiv:1205.5368 [hep-ph]].

Resources

- arXiv:1501.06858 Muon g-2 TDR, E 989
- particlebites.com
- Fermilab Resources
- YouTube resources (thank you Stanley Wojcicki, 2015 Panofsky Prize Winner "For his leadership and innovative contributions to experiments probing the flavor structure of quarks and leptons, in particular for his seminal role in the success of the MINOS neutrino oscillation experiment." f/o Susan, CEO of YouTube)
- April 7 talks of Aida X. El-Khadra and Chris Polly
- Quanta magazine
- Talk given by Gilberto Colangelo, Democritos Colloquium, April 20, 2021

- Quantum Electrodynamics formulated by Dirac, Pauli, Jordan, Feynman, Schwinger and Tomonaga
- Simplest theory with 2 parameters, m_e and α (Sommerfeld fine-structure constant)
- Extended to include other charged leptons, muon, and τ leptons, and charged quarks
- Free electron satisfies Dirac Equation (which contains the magnetic moment), g is the gyromagnetic ratio, $g = 2$ being the classical prediction of the Dirac theory.
- Feynman rules require us to have 'loops. At one-loop order, vacuum polarization, self-energy and vertex correction
- In general loops have to be 'regularized and the theory renormalized
- Vertex correction leads to the anomalous magnetic moment. $a_\mu \equiv (g-2)/2$

Experimental result on deviation from $g = 2$

PHYSICAL REVIEW VOLUME 74, NUMBER 3 AUGUST 1, 1948

The Magnetic Moment of the Electron†

P. KUSCH AND H. M. FOLEY
Department of Physics, Columbia University, New York, New York

(Received April 19, 1948)

A comparison of the g_J values of Ga in the $^2P_{3/2}$ and $^2P_{\frac{1}{2}}$ states, In in the $^2P_{\frac{1}{2}}$ state, and Na in the $^2S_{\frac{1}{2}}$ state has been made by a measurement of the frequencies of lines in the *hfs* spectra in a constant magnetic field. The ratios of the g_J values depart from the values obtained on the basis of the assumption that the electron spin gyromagnetic ratio is 2 and that the orbital electron gyromagnetic ratio is 1. Except for small residual effects, the results can be described by the statement that $g_L=1$ and $g_S=2(1.00119\pm0.00005)$. The possibility that the observed effects may be explained by perturbations is precluded by the consistency of the result as obtained by various comparisons and also on the basis of theoretical considerations.

1. INTRODUCTION

ONE of the important conclusions derived from the relativistic Dirac theory of the electron is that the electron possesses an angular momentum of $\frac{1}{2}$ measured in units of $h/2\pi$ and that with this angular momentum is associated a magnetic moment of one Bohr magneton. This conclusion substantiates earlier conclusions based on an analysis of the experimental data on the anomalous Zeeman effect. Indeed, all relevant experimental data have been in substantial agreement with this conclusion.

A direct measurement of the electron moment can most easily be made by a measurement of the g value of an atomic energy state. Direct determinations of the g values of atomic states from measurements of the frequencies of Zeeman lines in known magnetic fields, as, for example, in the work of Kinsler and Houston,[1] have yielded no significant differences between the measured atomic gyromagnetic ratios and the values consequent from the Dirac theory.* Millman and Kusch[2] have measured the magnetic moments of various nuclei, in particular that of the proton, in terms of the magnetic moment of the electron, assumed to be one Bohr magneton. The magnetic moments so found agree with those dependent on a measurement of a magnetic field in terms of classical standards to within about 0.14 percent ±0.5 percent. This again indicates that the g value of the electron is 2, to within the stated precision. It seems certain that any discrepancy with the theoretical value will be small.

The growth of various techniques of microwave and r-f spectroscopy makes available a series of new tools for the investigation of the detailed structure of atomic spectra. These techniques make it possible to resolve extremely minute details of structure and to determine the relative positions of energy levels to a very high degree of precision. The recent experiments of Lamb and Retherford[3] on the fine structure of hydrogen indicate that the Dirac theory does not adequately describe the hydrogen atom and that all the detailed conclusions of the Dirac theory are, therefore, presumably suspect to some degree.

In the recent measurements of Nafe, Nelson, and Rabi[4] of the hyperfine spectrum of the ground states of atomic hydrogen and deuterium, deviations of the zero field level splittings from the values predicted from theory were found. The theoretical values depend on a knowledge of the nuclear magnetic moment of the nucleus (known only in terms of an assumed value of the electron moment) as well as on the assumption that the magnetic moment of the electron is one Bohr magneton. Breit[5] has suggested that the discrepancy may be removed by the assumption that the electron possesses an "intrinsic" mag-

† Publication assisted by the Ernest Kempton Adams Fund for physical research at Columbia University.

[1] L. E. Kinsler and W. V. Houston, Phys. Rev. **45**, 104 (1934); **46**, 533 (1934).

* See, however, a consideration of these measurements in Section 6.

[2] S. Millman and P. Kusch, Phys. Rev. **60**, 91 (1941).

[3] W. E. Lamb, Jr. and R. C. Retherford, Phys. Rev. **72**, 241 (1947).

[4] J. E. Nafe, E. B. Nelson, and I. I. Rabi, Phys. Rev. **71**, 914 (1947). J. E. Nafe and E. B. Nelson, Phys. Rev. **73**, 718 (1948).

[5] G. Breit, Phys. Rev. **72**, 984 (1947).

The one-loop QED result from Schwinger

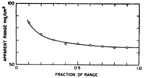

FIG. 2. Feather plot for Ca^{45}.

12,000 counts per minute, and the contribution due to gamma-rays and other unabsorbed contaminants was less than one part in 3000 with the strongest source, thus indicating the absence of any appreciable amount of gamma-radiation. The absorption curve obtained with the strongest source is shown in Fig. 1. The Feather plot, shown in Fig. 2, gives a range of 64 ± 1 mg/cm^2.

Glendenin[4] has shown that a reliable range-energy curve for the low energy region can be derived from the data of Marshall and Ward[5] for monoenergetic electrons and beta-ray spectrograph data on low energy beta-emitters. Glendenin's curve is identical with that of Marshall and Ward below 0.5 Mev. Using this range-energy curve, we have found that the Ca^{45} beta-radiation has a maximum energy of 260 ± 5 kev. We have found no evidence of any harder beta-radiation, or of any gamma-radiation at all in the course of this investigation.[6]

Acknowledgments.—This work has been supported with funds from the Office of Naval Research. The authors wish to express their appreciation to Miss Jacqueline Becker for her assistance in making the counts.

1 Walke, Thompson, and Holt, Phys. Rev. **57**, 171 (1940).
2 Solomon, Gould, and Anfinsen, Phys. Rev. **72**, 1097 (1947).
3 Feather, Proc. Camb. Phil. Soc. **35**, 599 (1938).
4 Glendenin, Nucleonics, in press for January, 1948.
5 Marshall and Ward, Can. J. Research **15**, 29 (1939).
6 This result is in good agreement with a value of 250 kev, given in *Radioisotopes, Catalog and Price List No. 2*, revised September, 1947, distributed by Isotopes Branch, United States Atomic Energy Commission. Unfortunately, the Atomic Energy Commission's result is not supported by any published experimental evidence.

On Quantum-Electrodynamics and the Magnetic Moment of the Electron

JULIAN SCHWINGER
Harvard University, Cambridge, Massachusetts
December 30, 1947

ATTEMPTS to evaluate radiative corrections to electron phenomena have heretofore been beset by divergence difficulties, attributable to self-energy and vacuum polarization effects. Electrodynamics unquestionably requires revision at ultra-relativistic energies, but is presumably accurate at moderate relativistic energies. It would be desirable, therefore, to isolate those aspects of the current theory that essentially involve high energies, and are subject to modification by a more satisfactory theory, from aspects that involve only moderate energies and are thus relatively trustworthy. This goal has been achieved by transforming the Hamiltonian of current hole theory electrodynamics to exhibit explicitly the logarithmically divergent self-energy of a free electron, which arises from the virtual emission and absorption of light quanta. The electromagnetic self-energy of a free electron can be ascribed to an electromagnetic mass, which must be added to the mechanical mass of the electron. Indeed, the only meaningful statements of the theory involve this combination of masses, which is the experimental mass of a free electron. It might appear, from this point of view, that the divergence of the electromagnetic mass is unobjectionable, since the individual contributions to the experimental mass are unobservable. However, the transformation of the Hamiltonian is based on the assumption of a weak interaction between matter and radiation, which requires that the electromagnetic mass be a small correction ($\sim(e^2/\hbar c)m_0$) to the mechanical mass m_0.

The new Hamiltonian is superior to the original one in essentially three ways: it involves the experimental electron mass, rather than the unobservable mechanical mass; an electron now interacts with the radiation field only in the presence of an external field, that is, only an accelerated electron can emit or absorb a light quantum;* the interaction energy of an electron with an external field is now subject to a *finite* radiative correction. In connection with the last point, it is important to note that the inclusion of the electromagnetic mass with the mechanical mass does not avoid all divergences; the polarization of the vacuum produces a logarithmically divergent term proportional to the interaction energy of the electron in an external field. However, it has long been recognized that such a term is equivalent to altering the value of the electron charge by a constant factor, only the final value being properly identified with the experimental charge. Thus the interaction between matter and radiation produces a renormalization of the electron charge and mass, all divergences being contained in the renormalization factors.

The simplest example of a radiative correction is that for the energy of an electron in an external magnetic field. The detailed application of the theory shows that the radiative correction to the magnetic interaction energy corresponds to an additional magnetic moment associated with the electron spin, of magnitude $\delta\mu/\mu=(\frac{1}{2}\pi)e^2/\hbar c=0.001162$. It is indeed gratifying that recently acquired experimental data confirm this prediction. Measurements on the hyperfine splitting of the ground states of atomic hydrogen and deuterium[1] have yielded values that are definitely larger than those to be expected from the directly measured nuclear moments and an electron moment of one Bohr magneton. These discrepancies can be accounted for by a small additional electron spin magnetic moment.[2] Recalling that the nuclear moments have been calibrated in terms of the electron moment, we find the additional moment necessary to account for the measured hydrogen and deuterium hyperfine structures to be $\delta\mu/\mu=0.00126\pm0.00019$ and $\delta\mu/\mu=0.00131\pm0.00025$, respectively. These values are not in disagreement with the theoretical prediction. More precise conformation is provided by measurement of the g values for the $^2S_{\frac{1}{2}}$, $^2P_{\frac{1}{2}}$, and $^2P_{3/2}$ states of sodium and gallium.[3] To account for these results, it is necessary to ascribe the following additional spin magnetic moment to the electron, $\delta\mu/\mu=0.00118\pm0.00003$.

$g-2$ at higher orders

- At one-loop, it is finite and was computed by Julian Schwinger to be $\alpha/(2\pi) \approx 0.00116$
- Heisenberg Uncertainty Principle $\Delta E \, \Delta t \geq \hbar$
- Think of loop as resulting from fluctuations of particle pairs from the vacuum
- The loops must account for all particles in nature and all interactions
- In the Standard Model these will include corrections with pairs of quarks, leptons, etc.
- Additional vertex will bring in 2 powers of e in loops and get suppressed
- As precision increases higher and higher loops must be accounted for
- Even though series in α is divergent we need to compute
- Electro-weak as well as loops with quarks.
- The latter cannot be computed in QCD
- High precision measurement vs. high precision calculations
- Beyond SM? Additional particles? Additional interactions?
- Supersymmetry? Extra-dimensions?

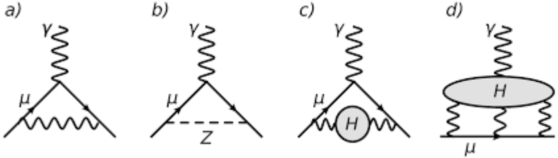
a)
γ
μ
b)
γ
μ
Z
c)
γ
μ
H
d)
γ
H
μ

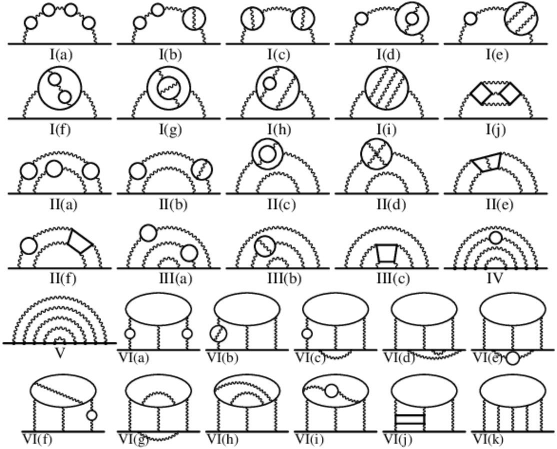
I(a)
I(b)
I(c)
I(d)
I(e)
I(f)
I(g)
I(h)
I(i)
I(j)
II(a)
II(b)
II(c)
II(d)
II(e)
II(f)
III(a)
III(b)
III(c)
IV
V
VI(a)
VI(b)
VI(c)
VI(d)
VI(e)
VI(f)
VI(g)
VI(h)
VI(i)
VI(j)
VI(k)

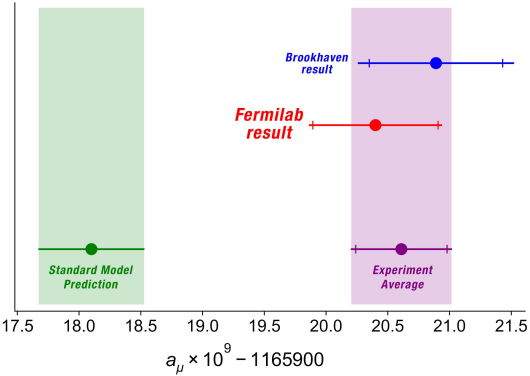
Brookhaven result
Fermilab result
Standard Model Prediction
Experiment Average
17.5
18.0
18.5
19.0
19.5
20.0
20.5
21.0
21.5
$a_\mu \times 10^9 - 1165900$

White Paper (2020): $(g-2)_\mu$, experiment vs SM

Contribution	Value $\times 10^{11}$
HVP LO (e^+e^-)	6931(40)
HVP NLO (e^+e^-)	$-98.3(7)$
HVP NNLO (e^+e^-)	12.4(1)
HVP LO (lattice BMW(20), *udsc*)	7075(55)
HLbL (phenomenology)	92(19)
HLbL NLO (phenomenology)	2(1)
HLbL (lattice, *uds*)	79(35)
HLbL (phenomenology + lattice)	90(17)
QED	116 584 718.931(104)
Electroweak	153.6(1.0)
HVP (e^+e^-, LO + NLO + NNLO)	6845(40)
HLbL (phenomenology + lattice + NLO)	92(18)
Total SM Value	116 591 810(43)
Experiment (E821)	116 592 089(63)
Difference: $\Delta a_\mu := a_\mu^{\rm exp} - a_\mu^{\rm SM}$	279(76)

- Hadronic Light by Light Scattering
- New dispersive calculation (Colangelo, Hoferichter, Procura, Stoffer)
- Very complicated calculation, with contributions from π, kaon, η, η
- Prior estimates coming from Nambu-Jona-Lasinio model, and lattice

Improvements obtained with the dispersive approach

Contribution	PdRV(09) *Glasgow consensus*	N/JN(09)	J(17)	WP(20)
π^0, η, η'-poles	114(13)	99(16)	95.45(12.40)	93.8(4.0)
π, K-loops/boxes	−19(19)	−19(13)	−20(5)	−16.4(2)
S-wave $\pi\pi$ rescattering	−7(7)	−7(2)	−5.98(1.20)	−8(1)
subtotal	88(24)	73(21)	69.5(13.4)	69.4(4.1)
scalars	–	–	–	} − 1(3)
tensors	–	–	1.1(1)	
axial vectors	15(10)	22(5)	7.55(2.71)	6(6)
u, d, s-loops / short-distance	–	21(3)	20(4)	15(10)
c-loop	2.3	–	2.3(2)	3(1)
total	105(26)	116(39)	100.4(28.2)	92(19)

- significant reduction of uncertainties in the first three rows: low-energy region well constrained by a dispersive approach

  CHPS (17), Masjuan, Sánchez-Puertas (17) Hoferichter, Hoid, Kubis, Leupold, Schneider (18)

- $1-2$ GeV and asymptotic region (short distance constraints) have been improved, but still work in progress (see WP(20))

  Melnikov, Vainshtein (04), (.......), Bijnens, Hermansson-Truedsson, Laub, Rodríguez-Sánchez (20,21)

Situation for HLbL

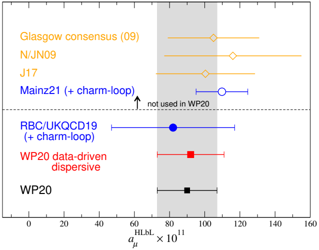

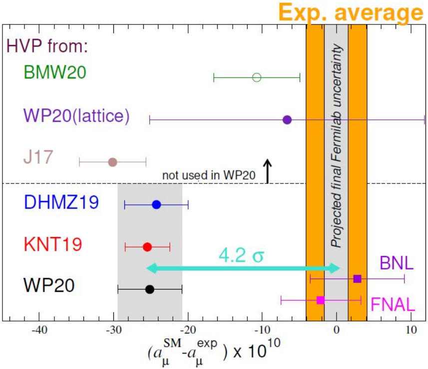
Exp. average
HVP from:
BMW20
WP20(lattice)
J17
not used in WP20
DHMZ19
KNT19
WP20
4.2 σ
Projected final Fermilab uncertainty
BNL
FNAL
-40
-30
-20
-10
0
10
$(a_\mu^{SM} - a_\mu^{exp}) \times 10^{10}$

$$a_\mu^{\pi\pi(\gamma),\,\mathrm{LO}}[\sqrt{t_l},\sqrt{t_u}] = \frac{\alpha^2 m_\mu^2}{12\pi^2}\int_{t_l}^{t_u}\frac{dt}{t}\,|F(t)|^2\,K(t)\,\beta_\pi^3(t)\,|F_\omega(t)|^2\left(1+\frac{\alpha}{\pi}\,\eta_\pi(t)\right)$$

- $F(t)$: the pion electromagnetic form factor in the isospin limit
- $K(t) = \int_0^1 du(1-u)u^2(t(1-u)+m_\mu^2 u^2)^{-1}$ the QED kernel
- $\beta_\pi(t) = (1-4m_\pi/t)^{1/2}$ two-pion phase space
- $F_\omega(t) = 1+\epsilon\frac{t}{(m_\omega - i\Gamma_\omega/2)^2 - t}$ isospin-breaking correction ($\omega-\rho$ mixing)
- $1+\frac{\alpha}{\pi}\,\eta_\pi(t)$: FSR correction (scalar QED)

Consider the low-energy contribution: $a_\mu^{\pi\pi(\gamma),\,\mathrm{LO}}[2m_\pi, 0.63\,\mathrm{GeV}] \equiv a_\mu$

Aim: reduce the error on a_μ by exploiting analyticity, unitarity and more precise phenomenological information on $F(t)$ available at other energies

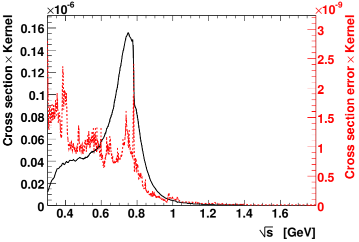

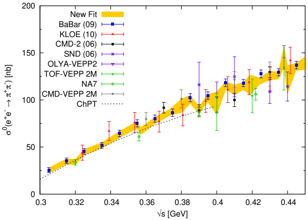

Davier et al. EPJ C**66**, 1 (2010) Hagiwara et al. J.Phys. G**38**, 085003 (2011)

- Left, black: combined data on the $e^+e^- \to \pi^+\pi^-$ cross section multiplied by the kernel function $K(s)$ in the integral for a_μ
- Left: red: corresponding error contribution, with statistical and systematic errors added in quadrature
- Right: low-energy data on the $e^+e^- \to \pi^+\pi^-$ cross section

Large experimental errors on the cross-section amplified by the QED kernel

$\Rightarrow$ More convenient to use the pion electromagnetic form factor

$$\langle \pi^+(p')|J_\mu^{\mathrm{elm}}|\pi^+(p)\rangle = (p+p')_\mu F(t), \;\; t = (p-p')^2$$

The theoretical motivation and strategy

- Largest theoretical error, $\delta a_\mu^{th} \sim 4.3 \times 10^{-10}$, from LO hadronic vacuum polarization (HVP)

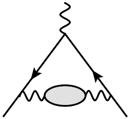

- A large part of it comes from the $\pi^+\pi^-$ contribution from low-energies
  - Compilation of e^+e^- data, including *BaBar* : Davier et al. (2010)

$$\boxed{a_\mu^{\pi\pi,\,\mathrm{LO}}\,[2m_\pi,\,0.63\,\mathrm{GeV}] = (133.2 \pm 1.3) \times 10^{-10}}$$

  - Integration of *BaBar* data alone: error $\sim 1.5 \times 10^{-10}$ Malaescu (2013)
  - Inclusion of KLOE 11: modest improvement, due to tension between *BaBar* and KLOE Hagiwara et al. (2011)
  - More recent experiments (KLOE 13, BESIII 16, CMD-3 preliminary) do not report data at low energies
- Before turning to our work, we review the experiment in the following

Experiments

- CERN experiments, 1960s large uncertainty
- Brookhaven National Laboratory - E821, end of the last century and early 21st century
- Fermilab Muon g-2 experiment, on going attempts to reduce uncertainty by a factor of 4
- Proposed experiment at JPARC in Japan using ultra-cold muons

Fermilab Muon $g-2$ experiment

Magnet

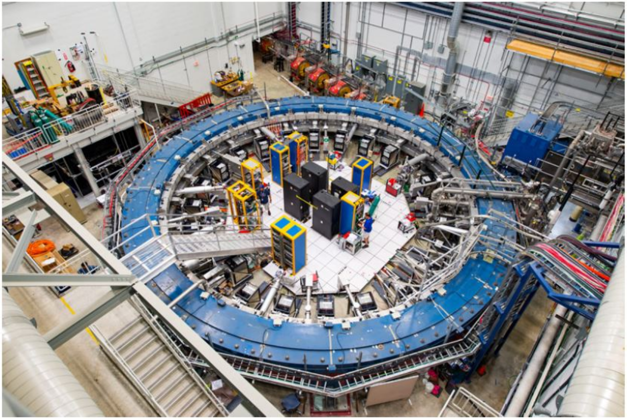

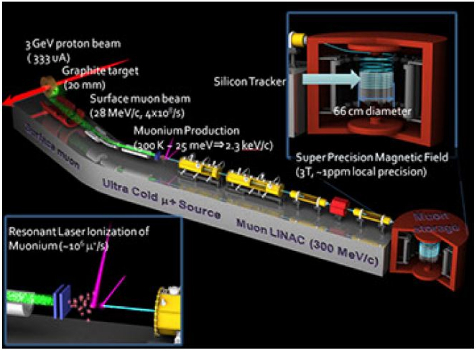
3 GeV proton beam
(333 uA)
Graphite target
(20 mm)
Surface muon beam
Muonium Production
Silicon Tracker
66 cm diameter
Super Precision Magnetic Field
(3T, ~1ppm local precision)
Surface muon
Ultra Cold μ+ Source
Muon LINAC (300 MeV/c)
Resonant Laser Ionization of

- Storage ring in which muons circulate at ‘magic energy
- muons produced from pion decay. $\pi^+(u\bar{d}) \rightarrow \mu^+ + \nu_\mu$ (produces polarized muons in direction of flight)
- $\mu^+ \rightarrow e^+\nu_e + \overline{\nu}_\mu$
- Uniform magnetic field in which muon polarisation vector precesses
- Decay of muon (parity violating weak decay) seen by infalling positron and correlated with polarisation by array of 24 Cherenkov detectors

The experimental apparatus

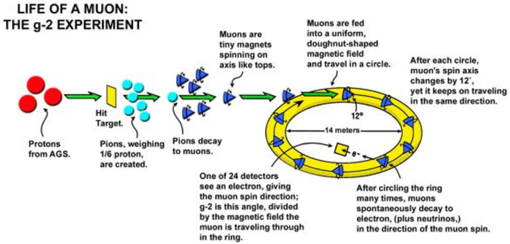

- $m_\mu = 105.65837755(23)$ MeV,
  $\tau_\mu = 2.1969811(22)\,\mu$s,
  $\alpha^{-1} = 137.035999174(35)$, 137.035999206 (the latter from Rubidium atom measurement, former from Caesium)
- $$\vec{\omega}_a = -\frac{e}{m}\left[a_\mu \vec{B} - \left(a_\mu - \frac{1}{\gamma^2 - 1}\right)\frac{\vec{B}\times\vec{E}}{c} - a_\mu \frac{\gamma}{\gamma+1}\left(\vec{\beta}\cdot\vec{B}\right)\vec{\beta}\right]$$
- We would like to tune the energy so that the second term can essentially be sent to 0. This is how we arrive at the magic energy. Recalling that $(\alpha/(2\pi) = 0.00116141)$ which is not needed at high precision for this purpose, the electric quadrupole field drops out of the spin-equations. The reason being that we do not know the electric field at sufficiently high precision. Now the result is dominated by the $\overline{B}$ field.

$$\gamma = \sqrt{1/a_\mu + 1} = 29.3602$$

$$\text{Magic Energy} = m_\mu \gamma = 3.10214\,\text{GeV},\ \tau = 64.5014\mu\text{s}$$

More on the experiments

- Energy and timing information
- Wiggle Plot from which ω_a is extracted
- Significant improvement compared to BNL at Fermilab, no hadronic flash, pions removed, protons removed, muon rate 3 times as high, more uniform B field, better focus
- Same magnet approximately 50 ft diameter magnet, $B = 1.45$ T uniform to 25 ppm
- Electric quadrupole field needed to keep muons in orbit and inside the storage rings

Arriving at the result

- Spinning muon, due to parity violation produces more charged decay daughter in direction of polarisation in terms of energy
- Since the muons are highly relativistic $\gamma \approx 29$ need to correct for the motion, with lifetime of about 64 microseconds
- Detectors are placed inside the annulus
- As the muon decays the charged daughter leaves the annulus and spirals in, as it no longer meets the cyclotron conditions
- Preferentially emitted (more energetic) along direction of polarisation

Wiggle Plot details

- As the polarisation vector precesses, the energy spectrum also changes as direction of the Lorentz boost makes an angle with the polarization vector gives rise to Wiggle Plot
- The Wiggle Plot allows us to measure the precession frequencyy ω_a
- Calorimeter measures total energy and incident position of positrons. Precise timing of decay positron to infer position of decaying muon. sub 100 ps precision on positron arrival time
- 10 MHz GPS disciplined master clock drives both ω_a and ω_p measurements
- 61.74 MHz field reference blinded by $\pm$25ppm
- All put together rate of detected positrons $E > E_{\rm thr}$
- $N(t) = N(0)\eta_N(t)\exp(-t/(\gamma\tau_\mu))\,[1 + A\eta_A(t)\cos(\omega_a t + \phi_0 + \eta_\phi(t))]$
- N_0 is a normalization $\gamma\tau_\mu \approx 64.4\mu$s, A is the average weak-decay asymmetry $\phi_0$is the esemble average phase angle, which depend on $E_{\rm th}$. η_i terms model effects due to betatron oscillations.

Wiggle

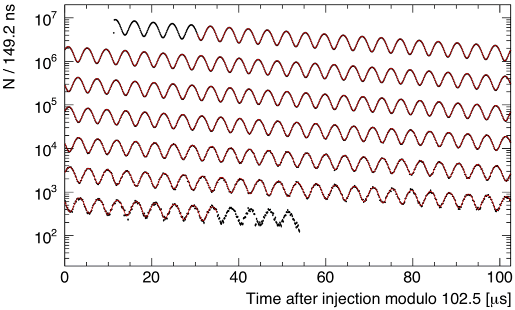

N / 149.2 ns
10^7
10^6
10^5
10^4
10^3
10^2
0
20
40
60
80
100
Time after injection modulo 102.5 [μs]

Summary of Experiments

- Based on all the above the observed precession frequency is measured at 434 ppb (statistical) and 56 ppb (systematic)
- Translated to muon magnetic moment at 0.46 ppm
- The results from the Fermilab Run 1 confirm the Brookhaven Result and are consistent with the same. The Fermilab central value is closer the SM central value. When the two are combined, we get a 4.2 σ deviation from the SM theory value.
- In the coming years, the data are expected to cut down the uncertainty by a factor of 4 compared to Brookhaven
- Improvements in the experiment and purity of the magnetic field

Improving the Pion Form factor

- The pion is a composite particle and contains u- and d-quarks/anti-quark pairs
- It is a complicated object and its coupling to a (virtual) photon is described by a form factor which is a function of the square of the energy
- At $t = 0$ it is normalized to unity in units of the electronic charge
- The cross-section for $e^+e^- \to \pi^+\pi^-$ is controlled by the form factor
- It is a complex function of the square of the energy with real and imaginary parts for $t > 4m_\pi^2$
- Unitarity is the property that relates the total-cross section to the imaginary part (optical theorem) of the forward scattering amplitude
- Unitarity also relates the phase of the form factor to that of the phase shift in elastic pion scattering (P- wave, Iso-spin=1) channel
- Analyticity is the property which says that the form factor if analytic in the cut energy squared phase with the cut running from threshold to infinity along the real energy square axis.
- The form factor is said to real analytic $F(t^*) = F^*(t)$
- Allows us to write a dispersion relation for the form factor itself: the full function can be reconstructed by $F(t) = 1/\pi \int_{4m_\pi^2}^{\infty} dt' \mathrm{Im} F(t')/(t'-t)$

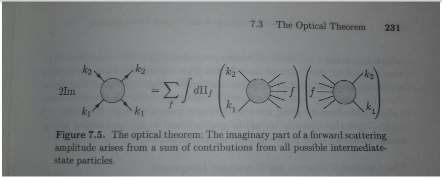

Figure 7.5. The optical theorem: The imaginary part of a forward scattering amplitude arises from a sum of contributions from all possible intermediate-state particles.

- The S-matrix: $S = 1 + iT$, with $SS^\dagger = 1 \implies 1 = 1 + i(T - T^\dagger + |T|^2)$
- $2\mathrm{Im}\, T = |T|^2 = (T^\dagger \sum_n |n\rangle\langle n| T)$ [Optical theorem]
- Cauchy's theorem

$$f(z) = \frac{1}{2\pi i} \oint \frac{f(z')}{z' - z}$$

- If the path is chosen to run along the real axis from $4m_\pi^2$ to ∞ (the branch cut) just above the axis, and then the circle completed and then runs parallel from ∞ to $4m_\pi^2$, with the contribution from the circle vanishing, we get the familiar dispersion relation given earlier
- Typically when integrals run along the square of the energy axis from threshold to ∞ they are called dispersive representation

Hadronic Vaccum Polarization Summary

Energy range	ACD18	CHS18	DHMZ19	KNT19
$\leq$ 0.6 GeV		110.1(9)	110.4(4)(5)	108.7(9)
$\leq$ 0.7 GeV		214.8(1.7)	214.7(0.8)(1.1)	213.1(1.2)
$\leq$ 0.8 GeV		413.2(2.3)	414.4(1.5)(2.3)	412.0(1.7)
$\leq$ 0.9 GeV		479.8(2.6)	481.9(1.8)(2.9)	478.5(1.8)
$\leq$ 1.0 GeV		495.0(2.6)	497.4(1.8)(3.1)	493.8(1.9)
[0.6, 0.7] GeV		104.7(7)	104.2(5)(5)	104.4(5)
[0.7, 0.8] GeV		198.3(9)	199.8(0.9)(1.2)	198.9(7)
[0.8, 0.9] GeV		66.6(4)	67.5(4)(6)	66.6(3)
[0.9, 1.0] GeV		15.3(1)	15.5(1)(2)	15.3(1)
$\leq$ 0.63 GeV	132.9(8)	132.8(1.1)	132.9(5)(6)	131.2(1.0)
[0.6, 0.9] GeV		369.6(1.7)	371.5(1.5)(2.3)	369.8(1.3)
$[\sqrt{0.1}, \sqrt{0.95}]$ GeV		490.7(2.6)	493.1(1.8)(3.1)	489.5(1.9)

Our Form Factor Analysis and Implications

- A full-fledged precision determination of the form factor, radius, and contribution to the $g-2$ in the low-energy region
- The charge radius squared is related to the slope at $t=0$ of the pion electromagnetic form factor $F(t)$,

$$F(t) = 1 + \frac{1}{6}\langle r_\pi^2 \rangle t + O(t^2)$$

- The most recent value of the pion charge radius, $r_\pi \equiv \langle r_\pi^2 \rangle^{1/2}$, quoted by PDG

$$r_\pi = (0.672 \pm 0.008)\,\mathrm{fm}, \tag{1}$$

- is obtained mainly from values of the form factor measured at small spacelike momenta $t < 0$ from
    - $e\pi \to e\pi$ and
    - $eN \to e\pi N$ processes,

  extrapolated to $t = 0$ using simple dipole-like parametrizations.
- ChPT at two-loop order (Bijnens et al., 1998) in the timelike region, $t > 0$, yields the best value $\langle r_\pi^2 \rangle = (0.437 \pm 0.016)\,\mathrm{fm}^2$, *i.e.* $r_\pi = (0.661 \pm 0.015)\,\mathrm{fm}$.
- The calculations in lattice QCD are consistent with these values, but have not yet reached the same precision (for a review, Aoki et al. 2017)

Strategy adapted for each of the problems

Basic idea:

- Use as input, instead of the modulus, the phase $\arg[F(t)]$, known with precision in the elastic region of the unitarity cut from Fermi-Watson theorem and Roy equations for $\pi\pi$ scattering
- Use additional, more precise, values of $F(t)$, available at other energies

Requirements on the method:

- No specific parametrization
- Independence on the unknown phase of $F(t)$ above the inelastic threshold
- Reliable evaluation of the errors

Achieved by using:

- Analyticity and unitarity of the form factor
- Adequate mathematical methods: extremal problems for analytic functions
- Statistical simulations to account for the uncertainties
- First applied to a_μ (BA, IC, DD and I. Sentitemsu Imsong, Physical Review D **93**, 116007 (2016))
- Now extended to radius and the form factor at specific energies

Extremal problem

Find optimal upper and lower bounds on the radius, for $F(t)$ in the class of functions real analytic in the t-plane cut along the real axis for $t \geq 4m_\pi^2$, which satisfy the following conditions:

- Phase known in the elastic region (from δ_1^1 phase-shift of $\pi\pi$ scattering):

$$\mathrm{Arg}[F(t+i\epsilon)] = \delta_1^1(t), \qquad 4m_\pi^2 \leq t \leq t_{in}$$

- An integral condition on the modulus squared above the inelastic threshold:

$$\frac{1}{\pi}\int_{t_{in}}^{\infty} dt\, w(t)\, |F(t)|^2 \leq I$$

- Given values for the first two Taylor coefficients at $t = 0$:

$$F(0) = 1, \qquad \left[\frac{dF(t)}{dt}\right]_{t=0} = \frac{1}{6}\langle r_\pi^2\rangle$$

- Given values at several spacelike and timelike energies:

$$F(t_n) = F_n \pm \epsilon_n, \qquad n = 1, 2...$$

Extremal problem

Find optimal upper and lower bounds on the radius, for $F(t)$ in the class of functions real analytic in the t-plane cut along the real axis for $t \geq 4m_\pi^2$, which satisfy the following conditions:

- Phase known in the elastic region (from δ_1^1 phase-shift of $\pi\pi$ scattering):

$$\mathrm{Arg}[F(t+i\epsilon)] = \delta_1^1(t), \qquad 4m_\pi^2 \leq t \leq t_{in}$$

- An integral condition on the modulus squared above the inelastic threshold:

$$\frac{1}{\pi}\int_{t_{in}}^{\infty} dt\, w(t)\, |F(t)|^2 \leq I$$

- Given values for the first two Taylor coefficients at $t=0$:

$$F(0) = 1, \qquad \left[\frac{dF(t)}{dt}\right]_{t=0} = \frac{1}{6}\langle r_\pi^2\rangle$$

- Given values at several spacelike and timelike energies:

$$F(t_n) = F_n \pm \epsilon_n, \qquad n = 1, 2\ldots$$

Combined phase-modulus problem. Can be reduced to a standard Schur-Carathéodory and Pick-Nevanlinna interpolation problem

Caprini, EPJC(2000), Abbas, Ananthanarayan, Caprini, Imsong and Ramanan, EPJA(2010)

Statistical simulations

- The formalism provides upper and lower bounds on radius at low energies for definite values of the input quantities (phase, charge radius, spacelike value, timelike modulus)
- To account for the uncertainties, we have generated a large number of pseudodata for each of the input quantities, using *a priori* given distributions (uniform or gaussian)
- We obtained a large sample ($\sim 10^6$) of values for the quantity radius for each timelike input
- The entire sample was binned to obtain a mean value and a 68.3% confidence level interval

Average of different experiments

- The prescription indicated a positive correlation between the values from different experiments
- The results from the two phases have been combined in a simple average
- The data from e^+e^- and τ-decay experiments are consistent in the region $0.65 - 0.71$ GeV $\Rightarrow$ the results from all 10 experiments can be combined into a single average:

$$r_\pi = (0.657 \pm 0.003)\,\text{fm}.$$

  The separate predictions obtained from e^+e^- and τ-decay data are (0.657 ± 0.003) fm and (0.658 ± 0.004) fm, respectively, showing that the average is dominated by the more precise e^+e^- data.
- The data from e^+e^- and τ-decay experiments are consistent in the region $0.65 - 0.71$ GeV $\Rightarrow$ the results from all 10 experiments can be combined into a single average:

$$a_\mu^{\pi\pi(\gamma),\,\text{LO}}[2m_\pi,\, 0.63\,\text{GeV}] = (133.258 \pm 0.723) \times 10^{-10}$$

Direct determination: $(133.2 \pm 1.3) \times 10^{-10}$ Davier et al. (2010)

- B. Ananthanarayan, I. Caprini and D. Das, "Test of analyticity and unitarity for the pion form-factor data around the ρ resonance," Phys. Rev. D **102** (2020) no.9, 096003 doi:10.1103/PhysRevD.102.096003 [arXiv:2008.00669 [hep-ph]].
- B. Ananthanarayan, I. Caprini and D. Das, "Pion form factor and low-energy hadronic contribution to muon $g-2$ by analytic extrapolation: consistency and sensitivity tests," Rom. J. Phys. **64** (2019) no.7-8, 401 [arXiv:1907.01767 [hep-ph]].
- B. Ananthanarayan, I. Caprini and D. Das, "Electromagnetic charge radius of the pion at high precision," Phys. Rev. Lett. **119** (2017) no.13, 132002 doi:10.1103/PhysRevLett.119.132002 [arXiv:1706.04020 [hep-ph]].
- B. Ananthanarayan, I. Caprini, D. Das and I. Sentitemsu Imsong, "Precise determination of the low-energy hadronic contribution to the muon $g-2$ from analyticity and unitarity: An improved analysis," Phys. Rev. D **93** (2016) no.11, 116007 doi:10.1103/PhysRevD.93.116007 [arXiv:1605.00202 [hep-ph]].

Summary of our work

- Strategy
  - The strategy was to use, instead of the modulus at low energies, the phase in the elastic region and measurements of the modulus outside the low-energy region
  - By solving a suitable extremal problem, upper and lower bounds on the radius have been obtained in a parametrization-free approach
  - The bounds are optimal and independent on the unknown phase of $F(t)$ above the inelastic threshold
  - The uncertainties of the input have been included by statistical simulations
- The result for the contribution to the charge radius 0.657 ± 0.003
- The error has been reduced by about a factor of 3
- The result for the contribution to $a_\mu^{\pi\pi,\,\mathrm{LO}}$ of energies below 0.63 GeV is consistent with the direct determination from combined e^+e^- data
- The error has been reduced by about 0.6×10^{-10} (a factor of 2)
- Some inconsistencies seen near the ρ in modulus measurement
- Very precise data even in a limited energy region allows precise extrapolation to other regions *without* specific parametrizations

Summary and Outlook

- The SM errors are dominated by the HVP and HLbL uncertainties
- Not much room for change. There is the possibility that HVP errors can shrink a little and the HLbL can be brought down to 10% from the present 20%
- BMW collaboration finds central value smaller than prior lattice determinations of HVP but with significantly lower errors
- The discrepancy remains an unresolved puzzle
- Possible improvement in cross-section measurements, improvements of HLbL data driven
- Improvements in lattice evaluations
- Fermilab experiment expected to lower BNL uncertainty by a factor of 4 (7σ discrepancy)
- SND, BES-III, CMD 3, BaBar
- HVP contribution dominates the uncertainty
- HLbL is numerically much lower than HVP but larger uncertainty
- Exciting times ahead